American Mineralogist, Volume 83, pages 58–67, 1998

Hydrothermal synthesis of ammonium illite

V. Šucha,[1]* F. Elsass,[2] D.D. Eberl,[3] L'. Kuchta,[4] J. Madejová,[5] W.P. Gates,[6] and P. Komadel[5]

[1]Department of Geology of Mineral Deposits, Comenius University, Mlynská dolina G, 842 15 Bratislava, Slovakia
[2]Station de Science du Sol, INRA, Route de St. Cyr, Versailles, France
[3]U.S. Geological Survey, 3215 Marine Street, Boulder, Colorado 80303-1066, U.S.A.
[4]Department of Inorganic Chemistry, Comenius University, Mlynská dolina, 842 15 Bratislava, Slovakia
[5]Institute of Inorganic Chemistry, Slovak Academy of Sciences, Dúbravská cesta 9, 842 36 Bratislava, Slovakia
[6]Division of Biogeochemistry, Savannah River Ecology Laboratory, University of Georgia, Drawer E, Aiken, South Carolina 29802, U.S.A.

Abstract

Synthetic gel and glass of illitic composition, natural kaolinite, and mixed-layer illite-smectite were used as starting materials for hydrothermal synthesis of ammonium illite. Ammonium illite was prepared from synthetic gel by hydrothermal treatment at 300 °C. The onset of crystallization began within 3 h, and well-crystallized ammonium illite appeared at 24 h. Increasing reaction time (up to four weeks) led to many illite layers per crystal. In the presence of equivalent proportions of potassium and ammonium, the gel was transformed to illite with equimolar contents of K and NH_4. In contrast, synthesis using glass under the same conditions resulted in a mixture of mixed-layer ammonium illite-smectite with large expandability and discrete illite. Hydrothermal treatments of the fine fractions of natural kaolinite and illite-smectite produced ammonium illite from kaolinite but the illite-smectite remained unchanged.

Introduction

Illite and interstratified illite-smectite are the most common clay minerals in claystones, shales, and hydrothermally altered volcanoclastic rocks. Illite itself, as well as the transformation of smectite to illite, has been extensively studied since the early 1960s. The illitic interlayer contains K as a fixed cation by definition but illites from different environments also have ammonium reported in the interlayers (Stevenson 1959 and other citations below). The content of ammonium can vary between several hundred parts per million to 100% for pure ammonium illite, which is called tobelite. The ammonium often comes from decomposition of organic matter in diagenetic environments (Cooper and Abedin 1981; Williams and Ferrell 1991; Compton et al. 1992) or from coal in anchimetamorphic environments (Juster et al. 1987; Daniels and Altaner 1990; Šucha et al. 1994). The source of ammonium is unclear in hydrothermally altered volcanoclastic rocks (Kozác et al. 1977; Higashi 1982; Bobos et al. 1995). Variable geological environments and the effect of parameters such as temperature, time, fluid, and solid composition on illite and illite-smectite formation have been investigated in many hydrothermal experiments (e.g., Eberl and Hower 1977; Eberl 1978; Roberson and Lahann 1981; Inoue 1983; Whitney and Northrop 1988; Güven and Huang 1991; Huang 1992; Eberl et al. 1993), but we found only one paper that focused on experimental ammonium illite formation (Shigorova et al. 1981).

This paper reports the results of hydrothermal synthesis of ammonium illite from synthetic gel and glass using different solid/fluid ratios. Also, natural kaolinite and illite-smectite were used as a starting materials. These minerals are common constituents of rocks and are often reported as ammonium illite precursors. Equivalent molar proportion of K and ammonium were used to document preferential incorporation into the illite structure.

Materials and methods

Starting materials

The following starting materials were selected for hydrothermal treatment: (1) synthetic gel of illitic composition, (2) synthetic glass of illitic composition, (3) <2 μm fraction of Sedlec kaolinite (Czech Republic), and (4) <2 μm fraction of mixed-layer illite-smectite mineral from the Dolná Ves hydrothermal deposit (Šucha et al. 1992), containing 34% expandable layers (ISCz-1, the Clay Minerals Society source clay repository).

Synthetic gels having compositions corresponding to the formula $[Si_{6.6}Al_{1.4}][Al_4](NH_4)_{1.4}O_{20}(OH)_4$ or $[Si_{6.6}Al_{1.4}][Al_4][(NH_4)_{0.7}K_{0.7}]O_{20}(OH)_4$ were prepared as follows. Silica colloidal powder was suspended in a solution of aluminum nitrate. Subsequently aluminum hydroxide was obtained by reaction with dilute ammonium hydroxide. This suspension was washed with distilled water until the

* E-mail: sucha@fns.uniba.sk

0003–004X/98/0102–0058$05.00

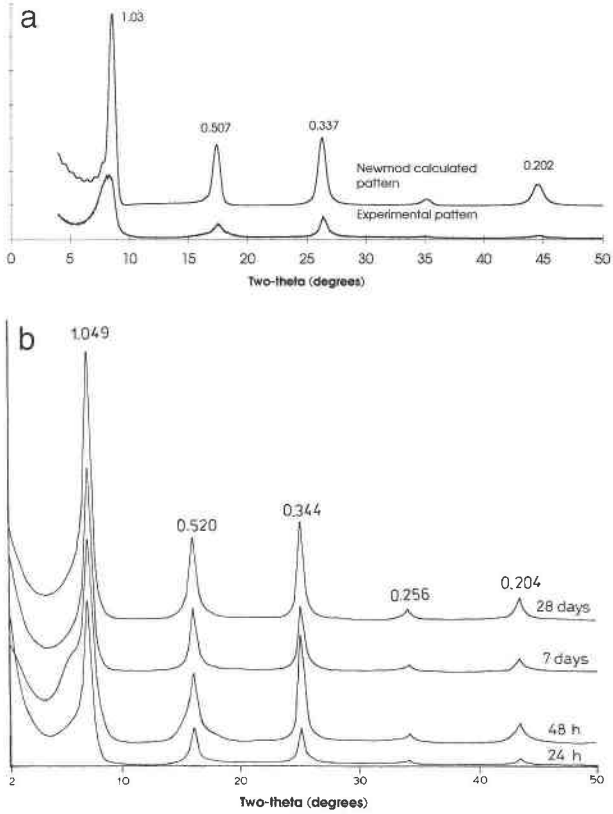

FIGURE 1. (**a**) XRD pattern of an experimental NH_4-K illite and calculated pattern of illite with equivalent molar contents of NH_4 and K in interlayers using NEWMOD program. (**b**) XRD patterns of ethylene-glycolated, oriented specimens from gel treated hydrothermally for 1, 2, 7, and 28 d.

nitrates were no longer detectable and then homogenized for 24 h. Finally ammonium hydroxide (in one experiment with potassium hydroxide) was added to the gel in amounts needed to obtain compositions corresponding to the structural formula.

A synthetic glass of the same composition as the NH_4-gel was prepared from silica colloidal powder suspended in a solution of aluminum nitrate, which was subsequently dried at 105 °C and calcined at 700 °C for 3 h. After calcination the glass was pulverized and ammonium hydroxide was added just before hydrothermal treatment. Natural illite-smectite and kaolinite were treated hydrothermally with ammonium hydroxide.

Hydrothermal treatment

The experiments were performed in autoclaves at 300 ± 5 °C for 3 h to 28 d using 50 mL Teflon containers. About 3 g of starting material was used for each experiment. The solid/water ratio was 1:1 for synthetic glass, kaolinite, and illite-smectite; however, the water content was much higher (about 90%) for the synthetic gel.

Characterization of the reaction products

The reaction products were characterized by X-ray diffraction (XRD), transmission electron microscopy

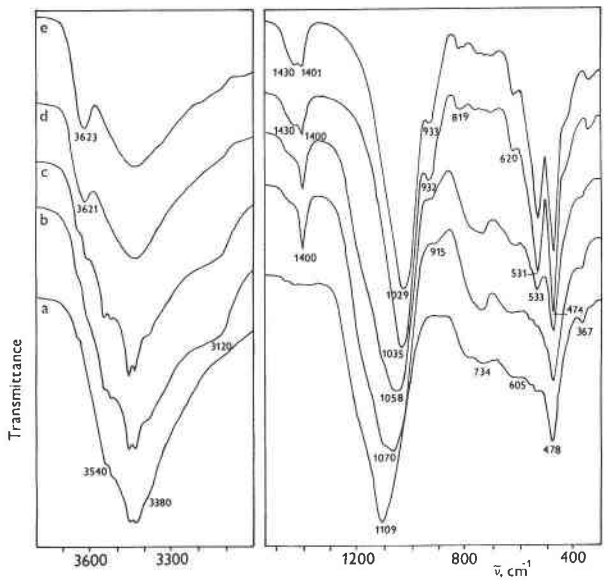

FIGURE 2. (**a**) IR spectra of amorphous gel, (**b**) samples after 3 h, (**c**) 6 h, (**d**) 24 h, and (**e**) 28 days synthesis in the 3800–3000 cm^{-1} (**left**) and 1550-3000 cm^{-1} (**right**) regions.

(TEM), high resolution electron microscopy (HRTEM), infrared spectroscopy (IR), and ^{29}Si magic-angle-spinning nuclear magnetic resonance spectroscopy (^{29}Si MAS NMR). Before XRD analyses, the reaction products were exchanged three times with 0.5 *M* $SrCl_2$ and subsequently dialyzed to exchange nonfixed cations. Then oriented specimens were prepared by sedimentation of the suspension on glass slides. Samples were analyzed in both air-dried and ethylene-glycolated (EG) states using a Siemens D-500 diffractometer (USGS, Boulder) equipped with a graphite monochromator and Cu$K\alpha$ radiation. The

TABLE 1. The ^{29}Si MAS NMR data of synthetic gel hydrothermally treated for 3 h, 24 h, and 3 weeks

Number	ppm	FWHH	% area	Assignments	Notes
			3 hours		
1	−62	1.3	1.1	Q^0(4Si) [$Si(Si)_4$]	1
2	−88.9	7.2	7.7	Q^4(4Al) and Q^4(2OH)	1,2
3	−95.8	12	65.5	Q^4(3Al)	1
4	−101.4	11	17.6	Q^4(2Al) and Q^4(1OH)	1,2
5	−105.6	3.3	5	Q^4(1Al)	1
6	−111.6	2.6	2	Q^4(0Al)	1
			24 hours		
1	−62	2	1.8	Q^0(4Si)	1
2	−83.8	4.1	10.8	Q^3(2Al)	3
3	−88.5	6.6	64.4	Q^3(1Al)	3
4	−93	4	23	Q^3(0Al)	3
			3 weeks		
1	−62	1.5	1.2	Q^0(4Si)	1
2	−87.6	8.7	76.7	Q^3(1Al)	3
3	−92.7	4.3	22.1	Q^3(0Al)	3

Notes: 1 = amorphous SiO_2, within parts per million range; 2 = substituted and hydrated SiO_4, within parts per million range, CP enhanced; 3 = substituted sheet SiO_0, within parts per million range, no CP enhancement. FWHH = full width at half height.

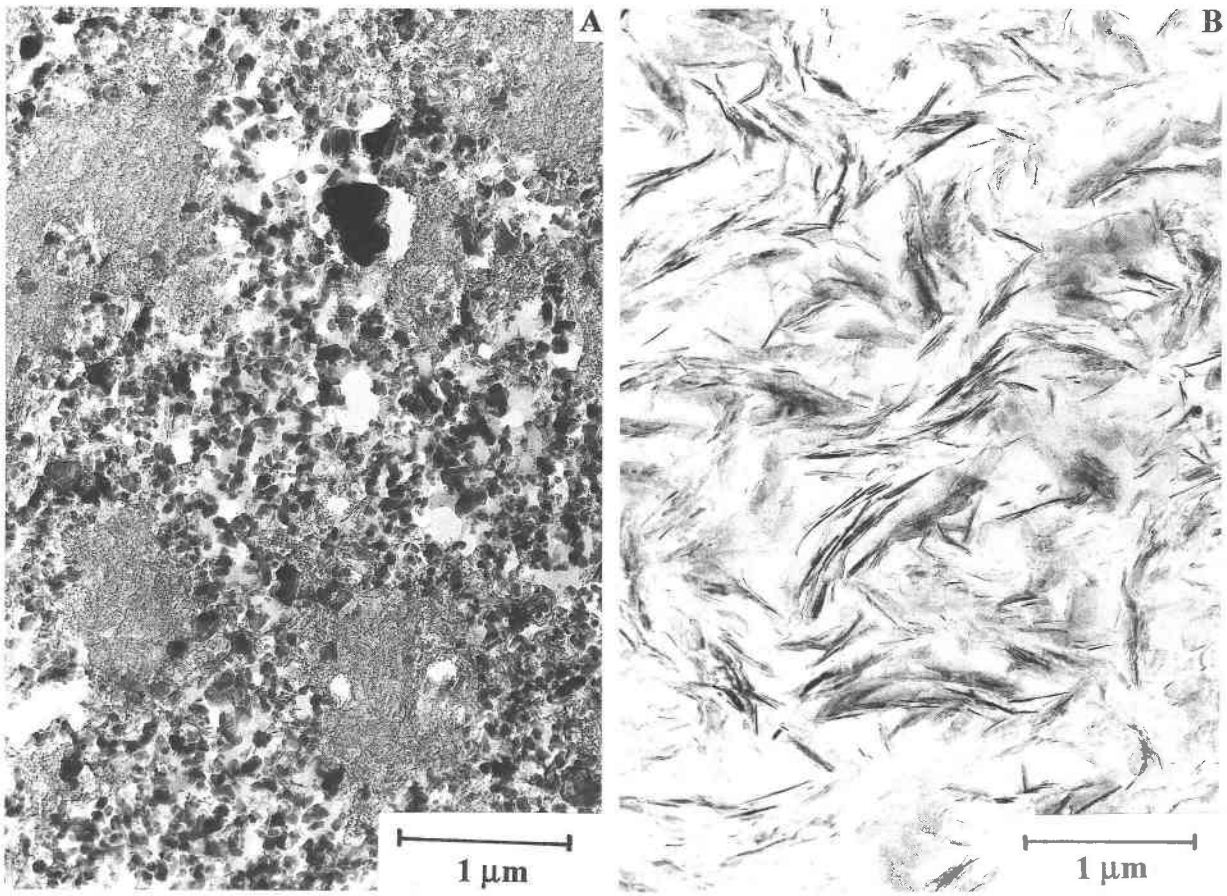

FIGURE 3. (A) TEM images at low magnification of reaction products after 3 h. (B) after 24 h of treatment.

proportion of expandable and non-expandable interlayers were determined using the NEWMOD computer program (Reynolds 1985) and calculated plots (Šucha and Širáňová 1991; Šucha et al. 1994).

Transmission electron microscopy (TEM) and high resolution transmission electron microscopy (HRTEM) measurements were performed using a Philips 420 STEM microscope operated at 120 kV. Two preparation procedures were used. Samples for TEM analysis were suspended in distilled water using an ultrasonic bath and then prepared by the sedimentation of the suspension onto copper grids already covered by collodium and carbon films. Samples were prepared for HRTEM analysis by coating with agar before applying the embedding procedure described by Tessier (1984). These samples were equilibrated with pure water at a pressure of 32 kPa. The water then was replaced by methanol and propylene oxide. Samples were subsequently impregnated with a Spurr resin. Ultrathin sections, 50 nm thick, were cut with a diamond knife on a Reichert Ultracut E microtome. During the embedding procedure, the swelling smectite interlayers were intercalated by organic components of the resin and d(001) was thus maintained at about 1.35 nm (Środoń et al. 1990). Only crystals having layers strictly parallel to the microscope axis display the images of the layer sequence. Pictures were taken in underfocus conditions close to the Scherzer defocus, and the use of an objective aperture eliminated lattice fringes smaller than 0.35 nm. Such one dimensional lattice fringes can be interpreted as representations of lattice images in which variations in stacking periodicities of crystals can be examined (Iijima and Buseck 1978). The numbers of layers in individual crystals and crystal thicknesses were measured, as described in detail by Środoń et al. (1990), on photographs taken at a magnification of 51000×. Thickness measurements were made from photos using a binocular microscope at a magnification between 10 and 40×.

IR absorption spectra were obtained on a Perkin-Elmer 983G spectrometer by using the KBr pressed disk technique (0.4 mg of sample and 200 mg of Kbr). Both single pulse (SP) and cross polarization (CP) nuclear magnetic resonance (NMR) experiments were conducted. All ^{29}Si MAS NMR spectra were collected at H_0 = 8.45 T (71.5 MHz) with a sample spinning frequency of 4.0 kHz on a GE300WB spectrometer. For single pulse experiments, up to 1800 acquisitions were collected with ratio frequency (r.f.) pulse times of 6 μs and 40 s recycle delay times. CP experiments were collected with r.f. pulse times of 8 μs, 2 s recycle delay times, and contact times of 2 ms.

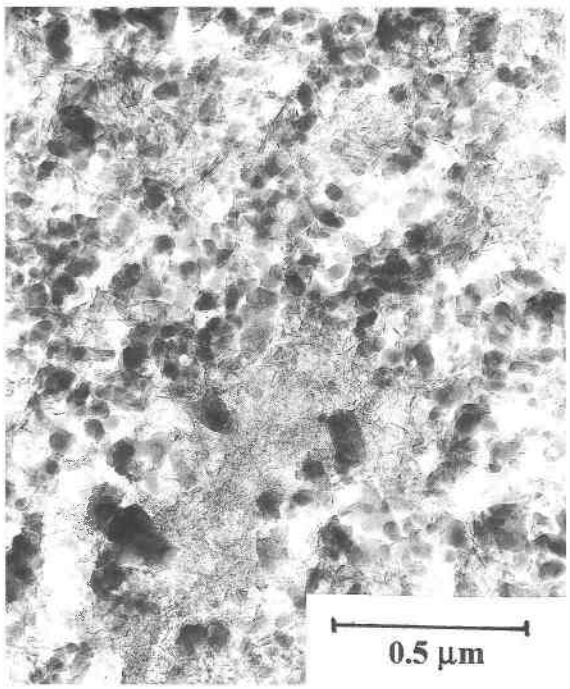

FIGURE 4. HRTEM image of 3 h treated gel at higher magnification displaying primitive clay layers.

The ^{29}Si chemical shifts were referred to tetramethylsilane (TMS). Spectral fitting of the SP spectra was accomplished using a curve analysis package (GEMCAP).

RESULTS

Hydrothermal treatment of the gel

Amorphous starting material of illitic composition was treated hydrothermally for periods from 3 h to 28 d. XRD patterns of the reaction products show a rapid evolution toward illitic structure. No reflections, only an elevated background in the 2θ range 15–30° 2θ, are present in the pattern of the 3 h experiment. The 6 h experiment shows only a broad low-angle shoulder at about 9° 2θ, which may indicate a 001 basal reflection for very thin illite. Significant changes were found between the 6 and 24 h products. The XRD pattern of the 24 h treated gel (Fig. 1) shows a set of sharp and well-defined peaks representing ammonium illite. The positions of the peak maxima were compared with those calculated by the NEWMOD program, and they fit well. Basically the XRD patterns were similar in all following experiments (48 h, 7 d, 14 d, 21 d, and 28 d; Fig. 1). No significant changes were observed even after EG saturation, except for the broad reflection at about 7.2° 2θ in the 24 and 48 h experiments, indicating the presence of some expandable interlayers. One 7 d experiment of the synthetic gel was conducted with equal amounts of K and ammonium. The reaction product was again illite. Its XRD pattern shows equivalent molar proportions of K (50%) and NH_4 (50%) in the illite interlayers (Šucha et al. 1994). The NEWMOD calculated XRD pattern of interstratified K-illite-

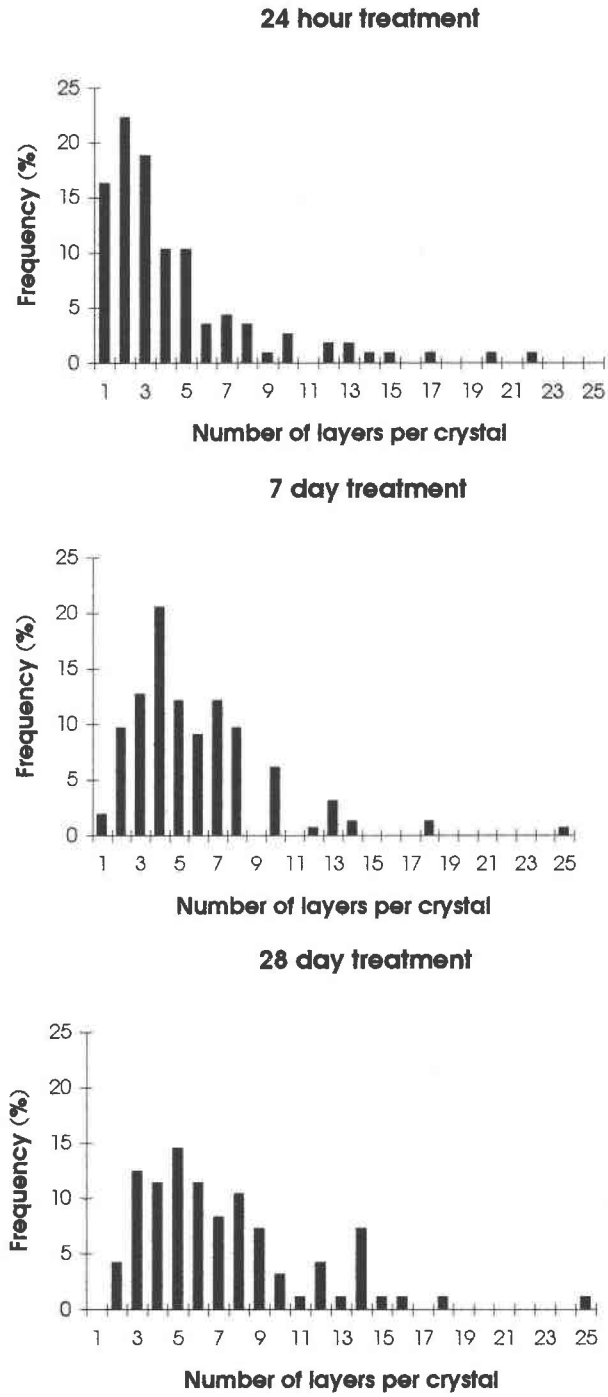

FIGURE 5. Histograms of the number of 2:1 layers per mixed-layer crystal in gels hydrothermally treated for 2, 7, and 28 d.

NH_4-illite replicates that obtained from the reaction product (Fig. 1a).

The IR spectrum of the starting material (Fig. 2a) shows a broad complex band near 3430 cm^{-1} containing the overlapping OH stretching bands because of $Al(OH)_3$ and of molecular H_2O. The OH pattern with shoulders

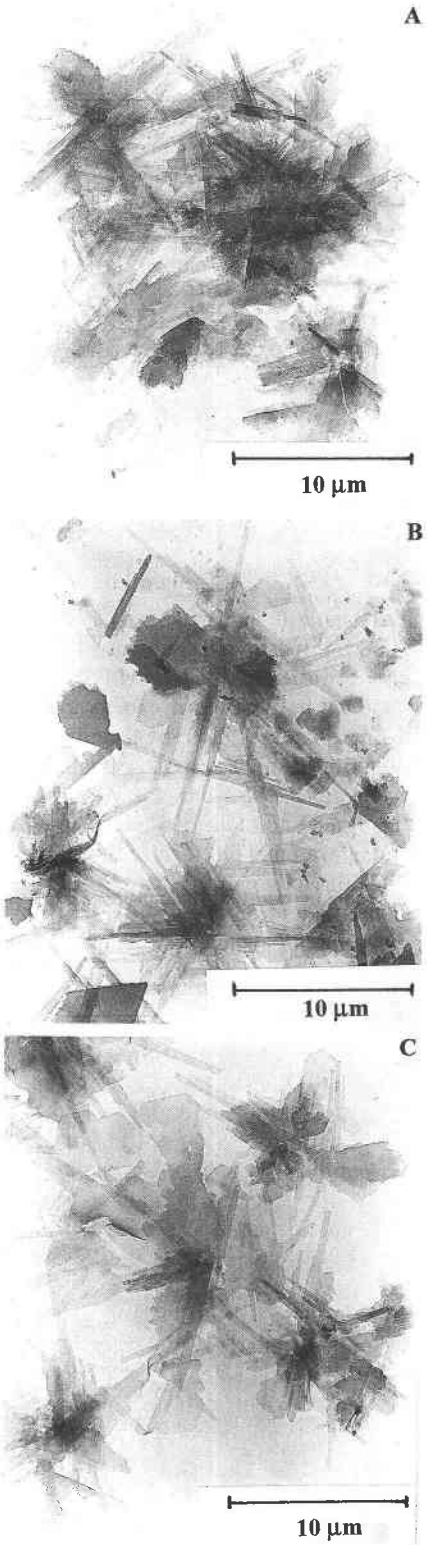

FIGURE 6. Transmission electron images of illite particles created by hydrothermal treatment of the gel for (**A**) 24 h, (**B**) 7 d, and (**C**) 28 d.

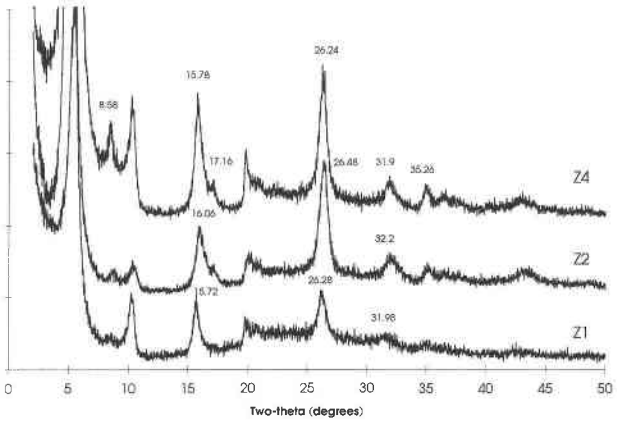

FIGURE 7. XRD patterns of ethylene-glycolated oriented specimens prepared from hydrothermally treated glass for (Z1) 7 d, (Z2) 14 d, and (Z4) 28 d.

near 3540 and 3380 cm^{-1} and with some splitting of the main band reflects the presence of an amorphous form of aluminum hydroxide. The sharp band at 367 cm^{-1} is also diagnostic for aluminum hydroxides (Russell and Fraser 1994). Broad absorption bands in the 800–500 cm^{-1} region are because of vibrations of aluminum hydroxide (Ryskin 1974). A strong band at 1109 cm^{-1}, assigned to Si-O stretching vibration, is typical for fourfold-coordinated silica (Moenke 1974). The position of the Si-O stretching band is very sensitive to the local environment of SiO_4 tetrahedra. Transformation of the three-dimensional Si framework to layered structure results in the shift of this band to lower frequencies. After the 3 h synthesis, the movement of the Si-O stretching band to 1070 cm^{-1} and the development of a shoulder near 915 cm^{-1} related to Al_2OH bending vibration confirms the formation of a layered structure (Russell and Fraser 1994; Fig. 2b). Further shift to 1058 cm^{-1} and the appearance of a new band at 533 cm^{-1}, attributed to Al-O-Si bending vibration, is seen in the spectrum after the 6 h of synthesis (Fig. 2c). This band is the most sensitive indicator of the presence or absence of octahedral aluminum in smectites (Breen et al. 1995). After the 24 h synthesis, all absorption bands characteristic for illite (i.e., the OH vibrations at 3621 and 932 cm^{-1} and the Si-O vibrations at 1035, 531, and 474 cm^{-1}) are observed in the IR spectrum (Fig. 2d). The absorption band at 819 cm^{-1} is because of Al-O out-of-plane vibration and reflects Al for Si substitution in the tetrahedral sheet (Russell and Fraser 1994). No significant changes were found in the 1100–300 cm^{-1} region in the interval between 24 h and four weeks (Figs. 2d and 2e). The presence of ammonium ions can be detected near 1400 cm^{-1} (Chourabi and Fripiat 1981). Both spectra of the samples after 3 and 6 h synthesis (Figs. 2b and 2c) show sharp bands at 1400 cm^{-1} and shoulders near 3120 cm^{-1} originating from the bending and stretching vibrations of NH_4, respectively. The shape of the band near 1400 cm^{-1} is changed in the spectrum of sample synthetized for 24 h (Fig. 2d). The band becomes broader

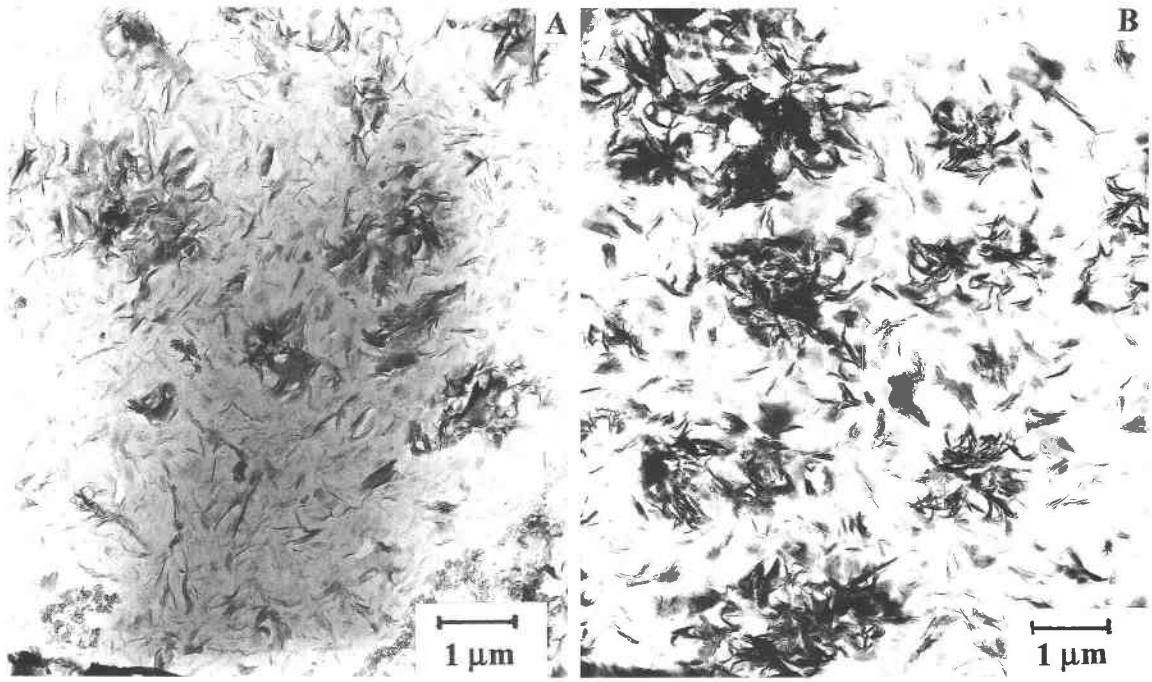

FIGURE 8. HRTEM images at low magnification of hydrothermally treated glass for (**A**) 7 d and (**B**) 28 d.

with two clearly resolved maxima at 1430 and 1400 cm^{-1} because of vibrations of NH_4 in the interlayers and in ammonium hydroxide, respectively (Chourabi and Fripiat 1981), thus confirming the development of a layered structure with NH_4 in the interlayers. The amount of interlayer NH_4 increases with increasing time of synthesis (compare the relative intensities of the bands at 1430 and 1400 cm^{-1} in the spectra of Figs. 2d and 2e). A relative increase in the amount of non-swelling layers in the sample synthetized for four weeks (Fig. 2e) is reflected in the higher intensity of the OH stretching band near 3620 cm^{-1} (Madejová et al. 1995). However, this sample still contains unreacted starting materials (see the low intensity absorption in the 850–700 cm^{-1} region).

With reaction time, a systematic decrease in both the overall line width and the number of fit components of the ^{29}Si MAS NMR spectra were observed. Six separate peaks were fit within the relatively broad spectrum of the sample treated for 3 h (Table 1), and all components represent Q^4 condensed and hydrated amorphous SiO_2 (Kirkpatrick et al. 1985). In the 3 h experiment, no indication of framework or sheet silicates existed. The fit components at −89 and −101 ppm were assigned to $Q^4(2OH)$ and $Q^4(1OH)$, respectively, because of the enhancement of these peaks relative to others in the CP experiment. These peaks also could be attributed to $Q^4(4Al)$ and $Q^4(2Al)$, respectively (Kirkpatrick et al. 1985). However, on the basis of the total amount of Al added to the system, these assignments are unlikely, specifically for the component at −89 ppm. The signal at −62 ppm is thought to be either fully condensed opal, $Q^0(4Si)$, i.e., $Si(Si)_4$ (Englehardt and Michel 1987) or possibly isolated Si tetrahedra (Lippmaa et al. 1980). The 24 h experiment shows condensation of the substituted and amorphous SiO_2 into three primary sheets or framework SiO_4-like phases. The assignments at −84, −88, and −93 ppm are assigned to $Q^3(2Al)$, $Q^3(1Al)$, and $Q^3(0Al)$, respectively (Englehardt and Michel 1987; Kirkpatrick et al. 1985; Kirkpatrick 1988). No significant change in the CP spectrum of the sample treated for 24 h was noted, thus ruling out the presence of any hydrated or OH-bearing phases. The results indicate that either an Al-substituted framework or dioctahedral sheet silicate began to form after only 24 h treatment. With further aging, the component at −84 ppm [peak associated with $Q^3(2Al)$] was lost while the contribution of the component at −88 ppm [peak associated with $Q^3(1Al)$] increased. The loss of the −84 ppm contribution was indicative of the condensation of Al-substituted Si phases into more Si-rich phases. No changes in chemical shift positions were noted with further aging beyond 24 h, except for a slight increase in the full width at half height (FWHH) for the −88 ppm component. Again, the lack of any increased intensity of the peaks during CP experiments rules out the possibility of assigning hydrated amorphous SiO_2 phases.

TEM images of the reaction products were taken from specimens prepared as ultrathin sections and suspensions. Images of the sections taken at low magnification (Fig. 3) show the evolution and arrangement of illite crystallites within 4 weeks of treatment. The marked difference is again between the 3 and 24 h experiment. A TEM image of the shortest experiment shows mostly amorphous starting gel, but also some homogeneous spots representing partly recrystallized matter. A higher magnifi-

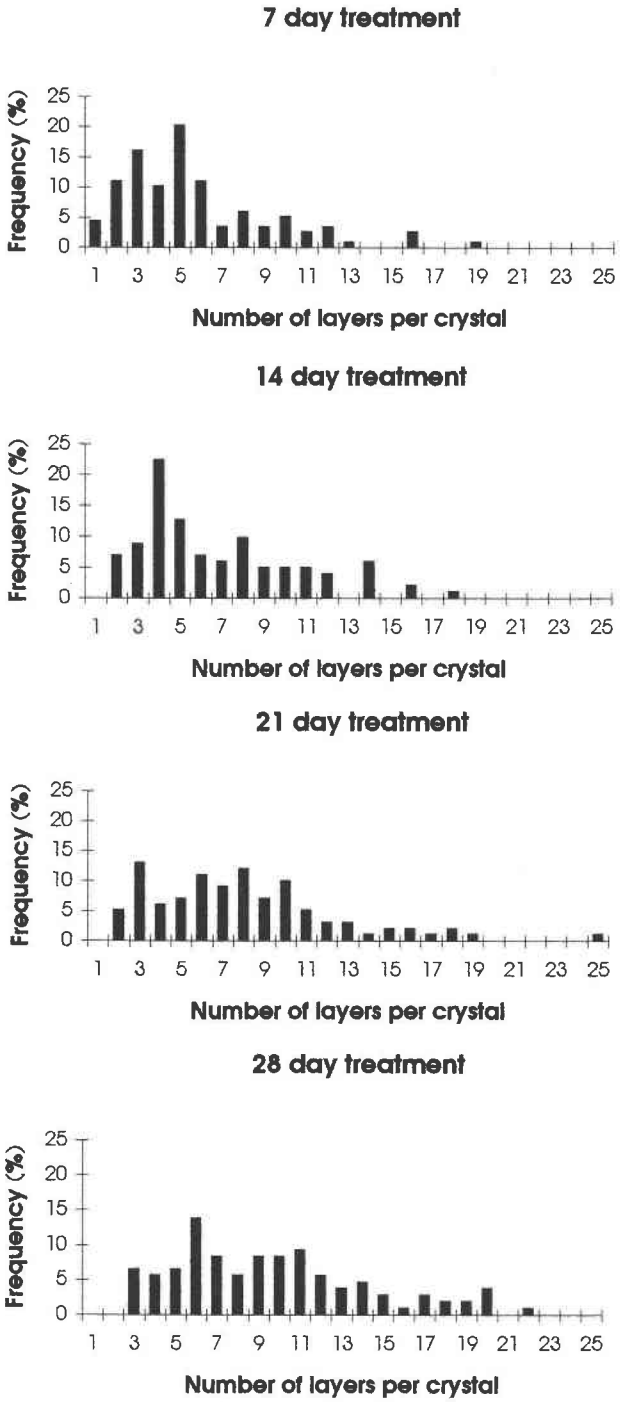

FIGURE 9. Histograms of the number of 2:1 layers per crystal of the glass treated for 7, 14, 21, and 28 days, respectively.

cation image of the same thin section (Fig. 4) confirms the existence of "primitive" very thin and short clay layers. The length of these layers is approximately 0.03 μm. They are invisible in the TEM images taken from specimens prepared by the suspension technique. The 24 h experiment image at low magnification is characterized by well-developed stacks of illite layers with a random arrangement. Only some changes in the HRTEM images, such as a small increase of the crystallite thickness and length of particles, with the time of the treatment are observed. Also, the amount of amorphous matter, represented by gray stains on the photographs, decreases with time of treatment. The number of layers per crystal at high magnification shows a small increase in the mean with the reaction time. The mean values were 4.4, 5.8, and 7.2 silicate layers per crystal for the 1, 7, and 28 d experiments, respectively. Histograms representing the distribution of 2:1 layers per crystal appear polymodal (Fig. 5) and indicate an evolution of crystal growth with increasing treatment. The histograms spread and their maxima are shifted toward higher values with increasing reaction time.

HRTEM images show very short stability of crystal fringes under the electron beam. Fringes were damaged easily by the electron beam within 2–3 min. The first step is a decrease of the *d* parameter from about 1.04 nm to 0.98 nm probably because of the release of ammonium from the illite interlayers. Only a few crystals have a *d* parameter smaller than 0.98 nm. Subsequently, some bubbles appear between individual fringes and finally fringes disappear.

The shapes of individual particles and aggregates were observed by using specimens prepared by the sedimentation of the clay suspension. As mentioned before, no clay particles were observed in the 3 h experiment. The 24 h experiment contains mostly lath particles, often arranged in sets 120° apart (Fig. 6), and some platy particles. The platy particles with hexagonal morphology became more common in the following experiments. Their microstructure shows three sets of laths oriented 120° apart on the bottom and an overgrowth of a new layer on the top. This crystal growth mechanism is called coalescence (Sunagawa et al. 1975).

Hydrothermal treatment of the glass

Glass as starting material was hydrothermally treated between 7 and 28 d. XRD patterns of the reaction products (Fig. 7) show differences compared to those obtained with the gel starting material. The XRD pattern of the product obtained from the shortest experiment, 7 d, shows a trace of a randomly interstratified mixed-layer NH_4-illite-smectite with a high smectitic content of about 90%. Also a small and diffuse reflection between 8 and 9° 2θ is observed, indicating the possible presence of ammonium illite. The 14 d experiment gives again a pattern of randomly interstratified NH_4-illite-smectite, however, with a much lower content of smectitic interlayers, 70–75%. Both the 21 and 28 d experiments give the same patterns showing an increase in the smectite content of the mixed-layer mineral (80–85%) and a significant increase in the intensity of the reflection at about 8.6° 2θ, representing a new mineral phase of ammonium illite.

TEM data of the ultrathin sections obtained at low magnification show randomly arranged, thin crystals and

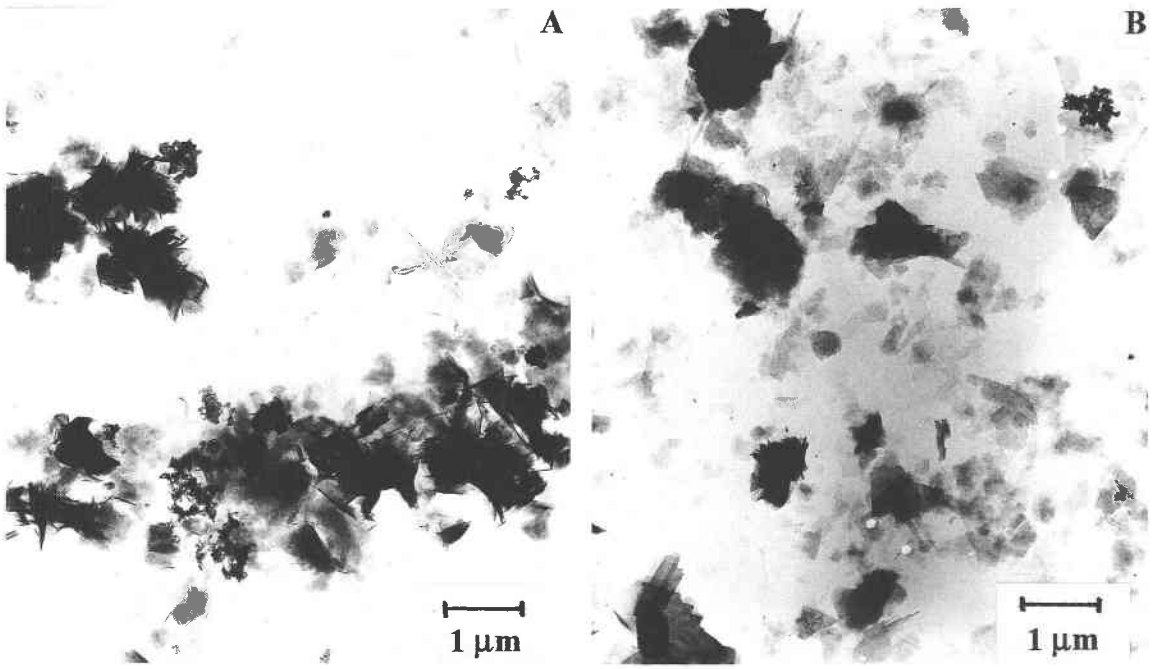

FIGURE 10. Transmission electron images of NH_4-illite and NH_4-illite-smectite particles originating from glass treated for (**A**) 7 d and (**B**) 28 d.

a lot of amorphous matter (Fig. 8) for the 7 d experiment. Products from 14 d of treatment show only small changes. The longest experiments (21 and 28 d) are very different from the previous ones. Mixed-layer crystals formed in three and four weeks are much thicker. The number of layers per one crystal, obtained at higher magnification on HRTEM images, confirms an increase in the mean thickness with the time of treatment: 5.7, 6.7, 8.4, and 9.6 layers per crystal for the 7, 14, 21, and 28 d treatments, respectively. Histograms of these measurements (Fig. 9) have a complicated polymodal distribution. TEM images obtained with the method of suspensions were used to determine the shape of the particles. Images of the 7 d experiment show predominantly foliated smectite-like flakes or aggregates of flakes with dimensions between 0.5 and 3 μm (Fig. 10). Rare small and extremely thin platy particles are present in this product. The longer experiments contain fewer curled flaky aggregates and more platy particles. In the 14 d experiment aggregates of thin laths arranged 120° apart were observed but they are not as common as in the products obtained from the treatment of the gel. Laths are rare in the 21 and 28 d experiments. Large and well-defined isometric particles (up to 4–5 μm) with distinct spots on selected-area electron diffraction pattern were found in the14 d experiment and then in all subsequent experiments. They are of a ribbon-like morphology. Many small particles (0.1–0.5 μm) of variable shapes (rhombs, laths, and particles with irregular outline) were found in the 14, 21, and 28 d experiments. They represent either individual particles or aggregates, often forming overgrowths on the foliated flakes. Particles of a characteristic hexagonal shape were absent.

Hydrothermal treatment of kaolinite and illite-smectite

A clay fraction of the kaolinite from Sedlec and mixed-layer illite-smectite from Dolná Ves were treated for 7 d under the same conditions as the gel and the glass. An XRD pattern of treated kaolinite shows well-defined reflections of ammonium illite and some traces of kaolinite precursor (Fig. 11). Thus kaolinite was transformed into illite very quickly. A different result was obtained when the reaction products of hydrothermally treated illite-smectite were analyzed. The XRD pattern shows no changes in the starting material within reaction time. Thus no ammonium was fixed in the smectitic interlayers and expandability measured after EG saturation remained unchanged after treatment.

INTERPRETATIONS AND CONCLUSIONS

Hydrothermal treatment was applied to synthetic amorphous gel and glass of the same chemical composition. Although these two starting materials differed only in physical state (gel vs. glass) and water/solid ratio, significant differences in the reaction products were found.

The gel was illitized quickly. Even within 3 h some changes were detected: HRTEM showed the existence of some primitive clay layers, and IR spectra showed shifts toward modes of the layered structure. After 24 h of treatment, a well-defined ammonium illite was identified. Longer treatment led to some changes in the particle arrangement and to an increase in the number of 2:1 layers

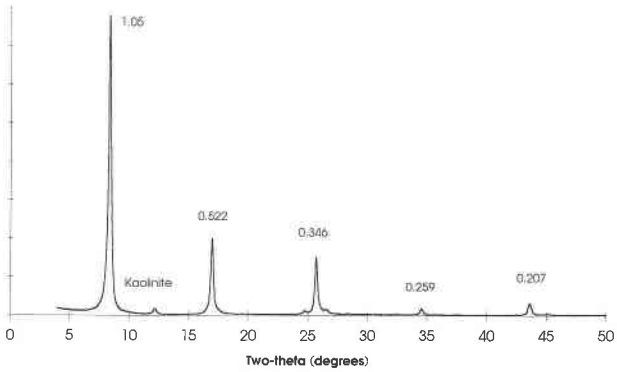

FIGURE 11. XRD pattern of NH_4-illite created by hydrothermal treatment of kaolinite.

per crystal. According to the TEM images, the first crystals to grow were laths of illite, which were mostly arranged in aggregates with the laths forming angles of 120°. There was subsequent overgrowth on the top of these laths (Fig. 6). In the first 1 to 2 d, nucleation and growth are the main growth mechanism, followed by crystal growth along *c* axis or coalescence. Direct illite crystallization from the gel shows that in environments with high water/solid ratio illite formation can be fast without a smectite or illite-smectite precursor.

Special attention was paid to synthesis of illite from amorphous gel in the presence of equivalent molar contents of ammonium and K. Both cations are common constituents of diagenetic and anchimetamorphic illites and illite-smectites (for references see introduction). The same proportion of K and NH_4 in the synthetic illite as in the starting materials implies that the proportion of these cations in natural illites reflects their availability during crystal growth. This hydrothermal evidence supports previous findings that there is no preferential fixation of K and ammonium in smectites during wetting and drying cycles (Šucha and Širáňová 1991).

Completely different products were found after hydrothermal treatment of the glass. A smectite-rich phase was formed, and longer treatments led to increased illitization. Therefore the illitization process is much more complicated than expected. Only 10% of the smectite is illitized within one week, forming randomly interstratified NH_4-illite-smectite. As illitization proceeded, about 25–30% of smectite was converted to ammonium illite after two weeks. At the same time, some traces of discrete illite appeared. Extended treatment led to further changes. Expandability of interstratified illite-smectite increased (probably because of an increase in the number of crystals per stack), and a significant amount of discrete NH_4-illite was formed. Probably several crystal growth mechanisms prevailed during the hydrothermal experiments with synthetic glass. The most common were nucleation of particles from the amorphous matter, dissolution of the nucleated particles, and precipitation of new ones. Coalescence, as observed on the TEM photographs, was a rare mechanism. The most interesting result is that both discrete illite and illite-smectite came into existence at the same time from the homogeneous material. It means that in natural environments we can expect at least three different phases of authigenic illite: illite from mixed-layer illite-smectite, illite crystallized directly from the source material, and illite transformed from other minerals, such as kaolinite. Fast illitization of kaolinite was also documented in one of the experiments.

ACKNOWLEDGMENTS

The authors thank L. Puškelová for XRD analyses. We greatly appreciate financial support of U.S.-Slovak Science and Technology Program (grant No. 92029).

REFERENCES CITED

Bobos, I., Šucha, V., and Soboleva, S. (1995) Mixed-layer ammonium illite-smectite and ammonium illite from hydrothermal system Hargita Bai, the East Carpathians (Romania). Book of Abstracts, 384 p. Euroclay 95, Leuven.

Breen, C., Madejová, J., and Komadel, P. (1995) Correlation of catalytic activity with infra-red, ^{29}Si MAS NMR and acidity data for HCl-treated fine fractions of montmorillonites. Applied Clay Science, 10, 219–230.

Chourabi, B. and Fripiat, J.J. (1981) Determination of tetrahedral substitutions and interlayer surface heterogeneity from vibrational spectra of ammonium in smectites. Clays and Clay Minerals, 29, 260–268.

Cooper, J.E. and Abedin, K.Z. (1981) The relationship between fixed ammonium-nitrogen and potassium in clays from a deep well on the Texas Gulf Coast. Texas Journal of Science, 33, 103–111.

Compton, J.S., Williams, L.B., and Ferrell, R.E. Jr. (1992) Mineralization of organogenic ammonium in the Monterey Formation, Santa Maria and San Joaquin basins, California, U.S.A. Geochimica at Cosmochimica Acta, 56, 1979–1991.

Daniels, E.J. and Altaner, S.P. (1990) Clay mineral authigenesis in coal and shale from the Anthracite region, Pennsylvania. American Mineralogist, 75, 825–839.

Eberl, D.D. (1978) The reaction of montmorillonite to mixed-layer clay: The effect of interlayer alkali and alkaline earth cations. Geochimica et Cosmochimica Acta, 42, 1–7.

Eberl, D.D. and Hower, J. (1977) The hydrothermal transformation of sodium and potassium smectite into mixed-layer clay. Clays and Clay Minerals, 26, 327–340.

Eberl, D.D., Velde, B., and McCormick, T. (1993) Synthesis of illite-smectite from smectite at Earth surface temperature and high pH. Clay Minerals, 28, 49–60.

Englehardt, G. and Michel, D. (1987) High-resolution solid state NMR of silicates and zeolites, 150 p. Wiley, New York.

Güven, N. and Huang, W.L. (1991) Effects of octahedral Mg^{2+} and Fe^{3+} substitutuions on hydrothermal illitization reaction. Clays and Clay Minerals, 39, 387–399.

Higashi, S. (1978) Dioctahedral mica minerals with ammonium ions. Mineralogical Journal, 9, 16–27.

——— (1982) Tobelite, a new ammonium dioctahedral mica. Mineralogical Journal, 11, 138–146.

Huang, W.L. (1992) Illitic-clay formation during experimental diagenesis of arkoses. In SEPM Special Publication, 47, 50–63.

Iijima, S. and Buseck, P.R. (1978) Experimental study of disordered mica structures by high-resolution electron microscopy. Acta Crystallographica, 34, 709–719.

Inoue, A. (1983) Potassium fixation by clay minerals during hydrothermal treatment. Clays and Clay Minerals, 31, 81–91.

Juster, T.C., Brown, P.E., and Bailey, S.W. (1987) NH_4-bearing illite in very low grade metamorphic rocks associated with coal, northeastern Pensylvania. American Mineralogist, 72, 555–565.

Kirkpatrick, R.J. (1988) MAS NMR spectroscopy of minerals and glasses. In Mineralogical Society of America Reviews in Mineralogy, 18, 341–403.

Kirkpatrick, R.J., Smith, K.A., Schramm, S., Turner, G., and Yang, W.H. (1985) Solid-state nuclear magnetic resonance spectroscopy of minerals. Annual Review of Earth and Planetary Sciences, 13, 29–47.

Kozác, J., Ocenás, D., and Derco, J. (1977) Ammonium hydromica from Vihorlat Mts. Mineralia Slovaca, 9, 479–494 (in Slovak).

Lippmaa, E., Mägic, M., Samoson, A., Englehardt, G., and Grimmer, A.R. (1980) Structural studies of silicates by solid-state high-resolution ^{29}Si NMR. Journal of American Chemical Society, 102, 4889–4893.

Madejová, J., Kraus, I., and Komadel, P. (1995) Fourier transform infrared spectroscopic characterization of dioctahedral smectites and illites from the main slovak deposits. Geologica Carpathica, Series Clays, 4, 23–32.

Moenke, H.H.W. (1974) Silica, the three-dimensional silicates, borosilicates and beryllium silicates. In V.C. Farmer, Ed., Infrared spectra of minerals, p. 365–382. Mineralogical Society, London.

Reynolds, R.C. (1985) NEWMOD, a computer program for the calculation of basal X-ray diffraction intensities and mixed-layered clays. R.C. Reynolds, Hanover, New Hampshire.

Roberson, H.E. and Lahann, R.W. (1981) Smectite-to-illite conversion rates: Effect of solution chemistry. Clays and Clay Minerals, 29, 129–135.

Russell, J.D. and Fraser, A.R. (1994) Infrared methods. In M.J. Wilson, Ed., Clay Mineralogy: Spectroscopic and chemical determinative methods, p. 11–67. Chapman and Hall, London.

Ryskin, Y.A.I. (1974) The vibrations of protons in minerals: hydroxyl, water and ammonium. In V.C. Farmer, Ed., Infrared spectra of minerals, p. 137–181. Mineralogical Society, London.

Shigorova, T.A., Kotov, N.V. Kotelnikova, Ye, N., Shamakin, B.M., and Frank-Kameneckiy, V.A. (1981) Synthesis, diffractometry, and IR spectroscopy of micas in the series from muscovite to the ammonium analog. Geochemistry International, 18, 76–82.

Środoń, J., Andreolli, C., Elsass, F., and Robert, M. (1990) Direct high-resolution transmission electron microscopic measurement of expandability of mixed-layer illite-smectite in bentonite rocks. Clays and Clay Minerals, 38, 373–379.

Stevenson, F.J. (1959) On the presence of fixed ammonium in rocks. Science, 130–221.

Sunagawa, I., Koshino, Y., Asakura, M., and Yamamoto, T. (1975) Growth mechanism of some clay minerals. Fortschritte der Mineralogie, 52, 217–224.

Šucha, V. and Širáňová, V. (1991) Potassium and ammonium fixation in smectites by wetting and drying. Clays and Clay Minerals, 39, 556–559.

Šucha, V., Kraus, I., Mosser, C., Hroncová, Z., Soboleva, K.A., and Širáňová, V. (1992) Mixed-layer illite-smectite from the Dolná Ves hydrothermal deposit, the Western Carpathians, Kremnica Mts. Geologica Carpathica-Series Clays, 43, 1, 13–19.

Šucha, V., Kraus, I., and Madejová, J. (1994) Ammonium illite from anchimetamorphic shales associated with anthracite in the zemplinicum of the western Carpathians. Clay Minerals, 29, 369–377.

Tessier, D. (1984) Étude experimental de l'organisation des materiaux argileux. Ph.D. thesis, 361 p. Universite Paris VII, INRA.

Whitney, G. and Northrop, H.R. (1988) Experimental investigation of the smectite to illite reaction: Dual reaction mechanisms and oxigen-isotope systematics. American Mineralogist, 73, 77–90.

Williams, L.B. and Ferrell, R.E. Jr. (1991) Ammonium substitution in illite during maturation of organic matter. Clays and Clay Minerals, 39, 400–408.

Manuscript received January 27, 1997
Manuscript accepted August 26, 1997